Variable property similarity transform: Application to axisymmetric fluid flow against a heated disk

David W. Weyburne
Air Force Research Laboratory, 80 Scott Drive, Hanscom Air Force Base, Massachusetts 01731
(Received 27 February 1998)

A variable property stream function is combined with a similarity variable transform to create a new class of variable property similarity transforms. The exact fluid flow solutions that are obtained with the new similarity transforms will be identical to the normally formulated similarity solutions. The utility of the new transforms will be for developing approximate analytical solutions. This is because the reformulation splits the normal transform into a slowly varying temperature functional and the rapidly temperature varying mass density. By assuming the functional is temperature invariant, approximate analytical solutions can be obtained by combining this approximate functional with a mass density profile approximation. The new approximate velocity solutions show the spatial variation behavior one would expect for a system with a temperature gradient present, in contrast to existing approximate methods that are based on average-property approximations. The new approximate analytical solutions, therefore, provide valuable insights into the expected thermal behavior and dependencies of the fluid system that cannot be obtained with exact numerical solutions or existing approximate methods. In addition, the approximate analytical solutions provide a straightforward path to the development of approximate thermal flow stability criteria. To demonstrate the utility of the new transform, the present study applies the new variable property similarity transform to the case of axisymmetric fluid flow against a heated disk. [S1063-651X(98)12112-8]

PACS number(s): 03.40.Gc, 47.20.Bp

I. INTRODUCTION

There are relatively few nontrivial exact solutions of the Navier-Stokes equations describing fluid flow. The two-dimensional and three-dimensional nature of most fluid systems makes even numerical solutions difficult to obtain. Similarity variable solutions are among the only known class of exact solutions to the equations of fluid motion. When simplifying assumptions that are appropriate to actual fluid behavior are combined with the similarity variable transform, the set of partial differential governing equations can be reduced to a set of ordinary differential equations. The numerical solutions to the transformed set of ordinary differential equations are, in general, so straightforward that the results are considered exact.

Most similarity variable transforms in the literature were initially developed as isothermal, fixed-property fluid descriptions. To include temperature effects, an energy balance equation, an energy equation of state, and appropriate boundary conditions are combined with the variable property mass and momentum balance equations. Applying the similarity transform to this combined set of equations results in a set of ordinary differential equations. The exact solutions to this set of governing equations are obtained one set at a time. Therefore it is not possible to make *a priori* predictions of the flow behavior for different flow conditions. Approximate solutions methods can make predictions to some degree using average-property approximations. However, because an average-property approximation is employed, the approximate velocity profiles obtained with this method do not show temperature-induced variations in the spatial directions. Without temperature-dependent spatial variations, it is not possible, for example, to predict the onset of thermally driven recirculations in the flow.

In the present study we describe a method for reformulating existing similarity transforms by incorporating the stream function into the transform. The exact solutions obtained by solving the set of differential equations using the new similarity transform are the same as for the normally formulated similarity transforms. The advantage of the new transform is that the velocity solutions are obtained in terms of the (mass) density profile and a set of transformed functions that are only weakly temperature dependent. By assuming the transformed functions are temperature independent, approximate analytical solutions can be constructed. Including the stream function, and thereby the mass continuity equation, into the transform means that a four-parameter analytical approximation is possible for these functions. The approximate transformed functions are then combined with an approximate density profile in order to obtain velocity approximations that exhibit temperature variations in the spatial directions. This temperature-dependent spatial variation is the main difference between the approximate solutions obtained herein and other approximate solutions that have appeared in the past. We demonstrate the new transform by applying the method to the one-dimensional model for flow against a heated disk.

No exact analytical solutions have been reported for the case of flow against a heated disk. For the limiting case of a system with the Reynolds number approaching infinity or zero, one can obtain simple polynomial approximations for the case where the rotation rate is zero, often referred to as stagnation point flow (see discussion and references in Houtman, Graves, and Jensen [1]). Recently, Dandy and Yun [2] applied the Kármán-Pohlhausen approximate solution method to this zero rotation case. For the rotating disk case, Hitchman and Curtis [3] discuss some simple linear analyti-

cal approximations useful in calculating surface concentration and temperature gradients. These approximations appear to be applicable for a very limited set of flow conditions. The rotating heated disk case is significant because this flow geometry is widely used in the chemical vapor deposition industry and in our laboratory [4]. Therefore this particular flow situation was chosen to demonstrate the utility of the new variable property similarity transform.

To obtain approximate analytical velocity profiles using the reformulated similarity transform technique discussed herein, the density profile must be known at least approximately. In general, this is not a problem since, for most of the similarity transforms that have appeared in the literature, the temperature profiles are already known at least approximately. However, for the case of gas flow against a heated rotating disk, it was necessary to develop an approximate expression for the density profile. A linear analytical expression in terms of the thermal boundary layer thickness was developed. Combining the analytical temperature profile with the reduced velocity approximations, we found that the resulting fluid description compares favorably to exact flow solutions for hydrogen, helium, and nitrogen gases flowing against a heated rotating disk.

In what follows, we begin with a review of the exact one-dimensional similarity transform for axisymmetric fluid flow against a heated disk. We then derive the new variable property similarity transform. To obtain the approximate analytical solutions for a heated rotating disk, we introduce a linear density profile approximation that is proportional to the boundary layer thickness. A general analytical expression for the boundary layer thickness is obtained from fits to experiment. The density profile approximation is then combined with a four-parameter spatial model to obtain velocity approximations. Finally, we discuss the results and point out how they can be used to generate flow stability criteria.

II. EXACT ONE-DIMENSIONAL FLUID FLOW MODEL

Steady-state fluid flow against a heated disk can be modeled theoretically by a combination of the Navier-Stokes equation, the energy balance equation, and the continuity equation. For an axisymmetric system, the continuity equation in cylindrical coordinates is

$$\frac{1}{r}\frac{\partial}{\partial r}\{\rho r V_r\}+\frac{\partial}{\partial z}\{\rho V_z\}=0, \tag{1}$$

where ρ is the density, V_r is the radial velocity, and V_z is axial velocity. Neglecting compressibility effects, the variable property axial component of the Navier-Stokes equation is given by

$$\begin{aligned}\rho V_r\frac{\partial V_z}{\partial r}+\rho V_z\frac{\partial V_z}{\partial z}&=\frac{\partial P}{\partial z}-\rho g+\frac{1}{r}\frac{\partial}{r}\left[\mu r\left(\frac{\partial V_z}{\partial r}+\frac{\partial V_r}{\partial z}\right)\right]\\&+\frac{\partial}{\partial z}\left[2\mu\frac{\partial V_z}{\partial z}-\frac{2}{3}\mu\left(\frac{1}{r}\frac{\partial}{\partial r}\{rV_r\}+\frac{\partial V_z}{\partial z}\right)\right],\end{aligned} \tag{2}$$

where P is the pressure, g is gravity acceleration, and μ is the viscosity. Similar expressions are obtained for the radial and circumferential components. To describe the fluid state fully, we must also include the energy balance. Neglecting viscous dissipation and absorption of radiation by the fluid, and assuming the heat capacity per unit mass c_p is constant, then the energy balance equation is given by

$$\rho V_r\frac{\partial T}{\partial r}+\rho V_z\frac{\partial T}{\partial z}=\frac{1}{c_p}\frac{\partial}{\partial r}\left(rk\frac{\partial T}{\partial r}\right)+\frac{1}{c_p}\frac{\partial}{\partial z}\left(k\frac{\partial T}{\partial z}\right), \tag{3}$$

where k is the thermal conductivity of the fluid and T is the temperature.

Given a set of boundary conditions and an equation of state relating P, ρ, and T, the above equations can be solved to obtain the fluid properties at any point in the system. However, the solutions at one point are obtained only after solving the governing equations over a grid of points spanning the boundaries. For a moderately complicated geometry, this grid can typically involve hundreds to thousands of points. Thus solving the set of partial differential equations becomes laborious and time consuming. One alternative is to reduce the set of three-dimensional (3D) partial differential equations to a set of 1D ordinary differential equations using a similarity variable transform. The one-time numerical solution to the set of ordinary differential equations is sufficient to define fluid properties at every point in the system.

von Kármán developed such a similarity transform to describe axisymmetric rotating disk flow [5]. Assuming that V_z, ρ, T, and μ are functions only of the axial coordinate z and that the radial velocity, the circumferential velocity (if applicable), and the radial pressure gradient are linearly dependent on the radial coordinate, then the von Kármán similarity transform can be employed:

$$\begin{gathered}\eta=z\sqrt{K/\nu_0},\\ V_r=rKf'(\eta),\quad V_\theta=r\Omega g(\eta),\quad V_z=-2\sqrt{K\nu_0}f(\eta),\end{gathered} \tag{4}$$

where the prime denotes derivative with respect to η, K and Ω are constants, $f(\eta)$ and $g(\eta)$ are dimensionless functions, and ν_0 is the kinematic viscosity. The von Kármán similarity transform can be applied to a number of flow situations by making various choices for K and Ω and the boundary conditions (see, for example, references in Ref. [6] and Evans and Greif [7]). As originally developed by von Kármán [5], the similarity transform for an infinite rotating disk is given by Eq. (4) with $K=\Omega=\omega$, where ω is the angular velocity of the disk.

III. VARIABLE PROPERTY SIMILARITY TRANSFORM

Recently, Evans and Greif [7] introduced a similarity variable for the geometry depicted in Fig. 1. If V_z^0 is the magnitude of the axial velocity of fluid exiting the injector, and L is the distance between the injector and the disk, then the new similarity variable is given by $K=\Omega=(\omega+V_z^0/L)$. In this geometry, the gas is ejected in a direction normal to the injector and onto the heated disk. For convenience, we locate the $z=0$ plane at the injector and the disk surface at the $z=-L$ plane. Fluid properties denoted with subscript or

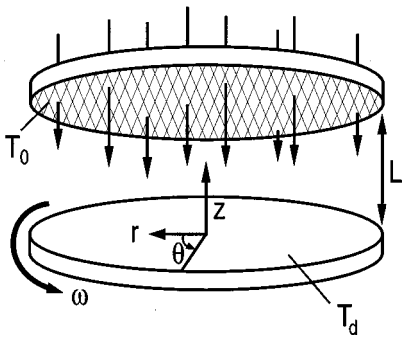

FIG. 1. Geometry and coordinate system. The fluid injector is located on the $z=0$ plane and the disk is located on the $z=-L$ plane. The gravity vector is parallel to the z axis.

superscript ''0'' thus refer to the initial fluid conditions. The injector and the disk are parallel and infinite in extent. In order to obtain variable property solutions, Evans and Greif [7] combined the variable property governing equations with a variable property similarity transform given by

$$\eta=(z+L)\sqrt{K/\nu_0},$$
$$V_r=rKF(\eta,T),\quad V_\theta=r\Omega G(\eta,T),\quad V_z=\sqrt{K\nu_0}H(\eta,T), \tag{5}$$

where $F(\eta,T)$, $G(\eta,T)$, and $H(\eta,T)$ are dimensionless functions and ν kinematic viscosity. By imposing the appropriate boundary conditions, the new transform can cover a large flow regime including stagnation point flow and infinite rotating disk flow.

Obtaining variable property numerical solutions to the set of governing equations [Eqs. (1)–(3)] is straightforward using the Evans and Greif similarity transform. In Fig. 2 the dimensionless axial velocity function $H(\eta,T)$ is plotted as a function of disk temperature for one set of flow conditions. While the exact solutions utilizing the similarity transform are simple and straightforward, there are a number of applications for which a reasonably accurate analytical approximation would be desirable. To develop approximate analytical expressions for the fluid situation described by Eq. (5), it would be necessary to develop approximations for the dimensionless functions $F(\eta,T)$, $G(\eta,T)$, and $H(\eta,T)$. There are two velocity boundary conditions each for V_θ, V_z, and V_r and two temperature boundary conditions. Thus a spatial variation approximation would be limited to a difficult two-parameter approximation. However, by reformulating the similarity equations using a stream function approach, the functions $F(\eta,T)$ and $H(\eta,T)$ can be combined into a new dimensionless function (see below). This new function can be readily approximated spatially with a four-parameter model. The problem is that there are no guidelines or boundary conditions as to how any of these dimensionless functions behaves with temperature.

One way of obtaining the temperature behavior of the dimensionless function $H(\eta,T)$, for example, would be to separate $H(\eta,T)$ into a weakly temperature-dependent function and a strongly temperature-dependent function. To accomplish this, we introduce a type of variable property similarity transform in which the reduced density appears explicitly in the transform. Assuming the spatial variation of the density can be estimated and that the new dimensionless

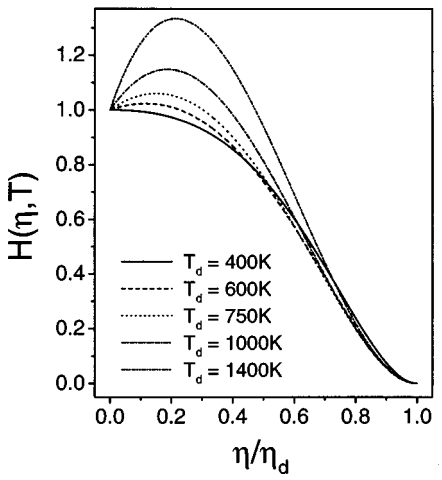

FIG. 2. Dimensionless axial velocity $H(\eta,T)$ at different disk temperatures. The simulated flow conditions are for hydrogen gas with $L=1.3$ cm, $P=152$ torr, $V_z^0=10.6$ cm/sec, $\omega=52$ radians/sec, disk temperature $T_d=400-1400$ K, and injector temperature $T_0=400$ K. The injector is located at $\eta/\eta_d=0$ and the disk is located at $\eta/\eta_d=1$.

function is relatively insensitive to temperature, the new transform allows us to introduce analytical approximations for $V_r(z,T)$ and $V_z(z,T)$ that exhibit temperature-gradient-induced variations in the z direction.

Our variable property similarity transform development is analogous to the fixed property case. We assume that V_z, ρ, and μ are functions only of the axial coordinate z and that the radial velocity, the circumferential velocity (if applicable), and the radial pressure gradient are linearly dependent on the radial coordinate. If the variable property stream function Ψ is given in terms of a dimensionless function $h(z,T)$ by

$$\Psi=\rho_0\sqrt{K\nu_0}r^2h(z,T), \tag{6}$$

then the continuity equation is automatically satisfied if

$$\rho(z,T)V_r(r,z,T)=-\frac{1}{r}\frac{d\Psi}{dz},$$
$$\rho(z,T)V_z(z,T)=\frac{1}{r}\frac{d\Psi}{dr}. \tag{7}$$

The function $h(z,T)$ that satisfies the above equations can be used to define a variable property similarity transform given by

$$\eta=(z+L)\left(\frac{K}{\nu_0}\right)^{1/2},$$
$$V_r=rK\frac{h'(\eta,T)}{\overline{\rho}(\eta,T)},\quad V_\theta=r\Omega G(\eta,T), \tag{8}$$
$$V_z=-2\sqrt{K\nu_0}\frac{h(\eta,T)}{\overline{\rho}(\eta,T)},$$

where $\overline{\rho}(\eta,T)=\rho(\eta,T)/\rho_0$.

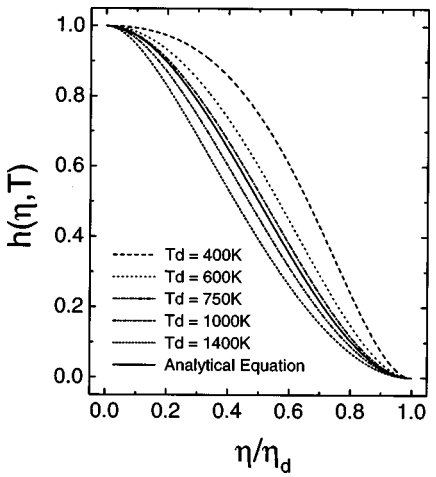

FIG. 3. Dimensionless axial velocity $h(\eta,T)$ for the variable property similarity transform at different disk temperatures. The simulated flow conditions and geometry are the same as those in Fig. 2. The solid line is the analytical approximation $c(\eta)$ given by Eq. (17).

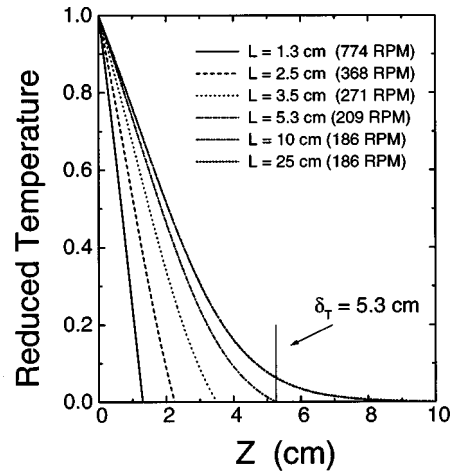

FIG. 4. Dimensionless temperature $(=\{T(z)-T_0\}/\{T_d-T_0\})$ as a function of the injector-to-disk spacing. The simulated flow conditions are for hydrogen gas with $P=152$ torr, $V_z^0=10.6$ cm/sec, disk temperature $T_d=1000$ K, and injector temperature $T_0=400$ K. The heated disk is located at $z=0$ and the injector is located at $z=L$.

The solutions of the set of differential equations describing the flow obtained by employing Eq. (8) will, of course, be identical to the solutions employing Eq. (5). Comparing the fixed and the variable property similarity transform given by Eqs. (4) and (8), we see that the function $h(\eta,T)/\overline{\rho(\eta,T)}$ reduces to $f(\eta)$ for the isothermal case. To illustrate the nature of the new transform, the new axial velocity function $h(\eta,T)$ is plotted in Fig. 3 for the same flow conditions used in Fig. 2. Comparing Figs. 2 and 3, it is evident that the temperature behavior of $h(\eta,T)$ is relatively weak compared to $H(\eta,T)$. It is not unreasonable, therefore, to approximate $h(\eta,T)$ by a function that is independent of temperature. This approximation should hold at least for a limited set of T_d, T_0, V_z^0, ω, and L values. Thus, if an approximation for the density profile were available, then it would be possible to obtain approximate velocity profiles for different disk temperatures.

IV. VELOCITY AND TEMPERATURE PROFILE APPROXIMATIONS

A. Temperature profile approximation

In order to develop analytical approximations for the flow velocities given in Eq. (8), an expression for the density profile $\rho(z,T)$ is needed. To approximate the density profile, we assume the fluid behaves as an ideal gas. Thus an approximate analytical expression for the temperature profile $T(z)$ will suffice. To develop an approximation, we first examined a series of exact temperature profile plots obtained by solving the governing equations using the variable property similarity transform [Eq. (8)]. In Fig. 4 we plot one sample set for hydrogen gas flow at different injector-to-disk gaps L. In this particular case, the rotation rate at each L is adjusted to mimic infinite rotating disk solutions, i.e., the condition $\partial P/\partial r=0$ was imposed. The temperature profiles in Fig. 4 for small L are well approximated by a linear line while the profiles for large L are essentially identical. At an intermediate point the flow changes from small L to large L behavior. The transition point roughly corresponds to the thermal boundary layer thickness δ_T, which, for this set of conditions, is about 5 cm. Assuming a linear model, the temperature profile is reasonably well approximated by

$$T(z)=\begin{cases} T_0-\Delta T z/L & \text{for } L<\delta_T \\ T_d-\Delta T(L+z)/\delta_T & \text{for } L\geqslant\delta_T \text{ and } z\leqslant(\delta_T-L) \\ T_0 & \text{for } L\geqslant\delta_T \text{ and } z>(\delta_T-L), \end{cases} \tag{9}$$

where $\Delta T=T_d-T_0$. We now have a reasonable approximation of the temperature profile, and therefore the density profile, with only one unknown, the boundary layer thickness.

B. Thermal boundary layer thickness

Thermal and momentum boundary layer thicknesses are terms usually applied to flow in which bulk flow properties persist up to a thin layer adjacent to a physical boundary. For the flow situation described by Evans and Greif's similarity variable, this condition is only fulfilled for a small subset of T_d, T_0, V_z^0, ω, and L which mimic an infinite rotating disk. The isothermal expression for the momentum boundary layer thickness δ_m of an infinite rotating disk [8] is given by

$$\delta_m \propto \sqrt{\nu_0/\omega}. \tag{10}$$

From a simple heat transfer argument, Schlichting [8] has shown that the momentum and thermal boundary layer thicknesses are approximately related by the expression $\delta_m \sim \delta_T \mathrm{Pr}^{1/2}$, where Pr is the Prandlt number. Therefore the thermal boundary layer thickness is given by

$$\delta_T \propto \sqrt{\nu_0/\omega \mathrm{Pr}}. \tag{11}$$

Examination of Eq. (11) indicates that the thermal boundary layer thickness does not depend on the disk temperature. To verify that this is indeed the case for the heated disk, we generated a large set of similarity solutions by varying the independent variables. To ensure that the solutions had true boundary layer behavior, only those solutions for zero radial

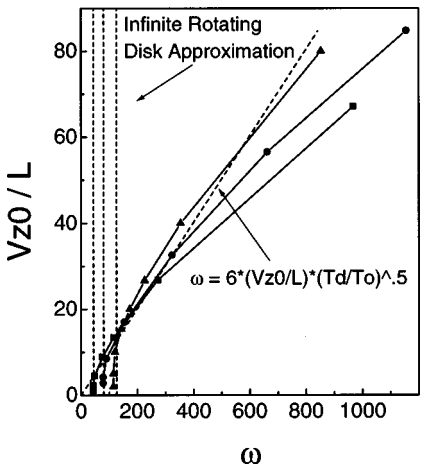

FIG. 5. Exact solutions to the governing equations for the case where $\partial P/\partial r=0$. The circles are for hydrogen gas with $L=0.5-45$ cm, $P=760$ torr, $V_z^0=2.12$ cm/sec, $T_d=1400$ K, and $T_0=400$ K. The triangles are for nitrogen gas with $L=0.5-10$ cm, $P=152$ torr, $V_z^0=5$ cm/sec, $T_d=750$ K, and $T_0=400$ K. The squares are for helium gas with $L=0.5-15$ cm, $P=620$ torr, $V_z^0=5.47$ cm/sec, $T_d=700$ K, and $T_0=300$ K. The vertical dashed lines are generated using the infinite rotating disk expression given by Breiland and Evans [9]. The dashed linear line was obtained as a best manual fit to a series of similar plots.

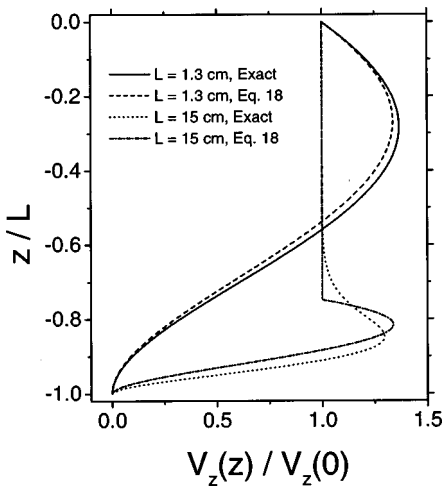

FIG. 6. Comparison between the approximate analytical solutions and the exact solutions to the governing equations for the axial velocity profile. The rotation rate in each case is adjusted so that $\partial P/\partial r=0$. For the two $L=1.3$ cm lines, the simulated flow conditions are the same as those used in Fig. 2 with $T_d=1000$ K. The other two lines are the exact and the approximate solutions for the same conditions but with $L=15$ cm.

pressure gradient, i.e., $\partial P/\partial r=0$, were considered. After examining many data sets in which we would vary one variable and keep all but one of the other variables constant, we found that the similarity variable quantities V_z^0, L, and ω are the key parameters that determine the flow behavior. In Fig. 5 we plot the quantities V_z^0/L versus the rotation rate ω for a number of gases and conditions. The vertical dashed line in the plot is generated using the approximate analytical expression for V_z^0 of an infinite rotating disk given by Breiland and Evans [9]. We obtained the dashed linear line in the plots as a best manual fit to a whole series of plots using different gases and conditions [10]. This equation is given by

$$\frac{V_z^0}{\omega L}\cong\frac{1}{6}\left(\frac{T_0}{T_d}\right)^{1/2}. \tag{12}$$

This relationship establishes the conditions for which $\partial P/\partial r=0$ in the temperature range of our analysis, $400\ \mathrm{K}\leqslant T_d\leqslant 1400$ K. So far we have only tested it for helium, nitrogen, and hydrogen gases, but we believe it will work for most gases with similar Prandlt numbers.

Examination of the plot reveals that the boundary thickness δ_m may be taken as the intersection of the straight line given by Eq. (12) and the infinite rotating disk expression generated from the Breiland and Evans [9] expression. Thus

$$\delta_T\cong 6\,\frac{\nu_0}{V_z^0\sqrt{\mathrm{Pr}}}\left[H^2(\infty)\left(\frac{T_d}{T_0}\right)^{1/2}\right], \tag{13}$$

where $H(\infty)$ is Breiland and Evans's analytical approximation. The quantity in square brackets represents the effect of temperature on the traditional boundary layer expression [Eq. (11)]. For hydrogen gas, the quantity in parentheses varies from 0.75 at 400 K to 1.1 at 1400 K. The boundary layer thickness is indeed only weakly dependent on the temperature.

C. Approximate analytical velocity expression

With the boundary layer thickness given by Eq. (13), we now have an approximate density profile for the rotating disk case. We now determine a temperature-independent approximation for the function $h(\eta,T)$. From examination of Fig. 2, we assume a trial solution of the form

$$h(\eta,T)\approx c(\eta)\equiv a_1+a_2\eta+a_3\eta^2+a_4\eta^3. \tag{14}$$

The boundary conditions for this transformed system at $\eta=0$ are

$$h(\eta,T)\big|_{\eta=0}=\frac{V_z^0}{2\sqrt{K\nu_0}},\quad h'(\eta,T)\big|_{\eta=0}=0 \tag{15}$$

and at the disk, $\eta=\eta_d$,

$$h(\eta,T)\big|_{\eta=\eta_d}=0,\quad h'(\eta,T)\big|_{\eta=\eta_d}=0. \tag{16}$$

Applying the same boundary conditions to $c(\eta)$, we find

$$c(\eta)=\frac{V_z^0}{2\sqrt{K\nu_0}}\left(1-3\,\frac{\eta^2}{\eta_d^2}+2\,\frac{\eta^3}{\eta_d^3}\right). \tag{17}$$

This analytical expression is compared to the exact calculation of $h(\eta,T)$ in Fig. 3. An approximate analytical solution is obtained by combining Eq. (17) and the approximate density profile. Thus

$$V_r(r,z,T)\cong\begin{cases} -r\,\dfrac{3V_z^0}{\overline{\rho}(z,T)}\left\{\dfrac{z}{L^2}+\dfrac{z^2}{L^3}\right\} & \text{for } L<\delta_m \\ -r\,\dfrac{3V_z^0}{\overline{\rho}(z,T)}\left\{\dfrac{z-\delta_m+L}{\delta_m^2}+\dfrac{(z-\delta_m+L)^2}{\delta_m^3}\right\} & \text{for } L\geqslant\delta_m \text{ and } z\leqslant(\delta_m-L) \\ 0 \quad \text{for } L\geqslant\delta_m \text{ and } z>(\delta_m-L), \end{cases}$$

$$V_z(z,T)\cong\begin{cases} \dfrac{V_z^0}{\overline{\rho}(z,T)}\left\{\dfrac{3z^2}{L^2}+\dfrac{2z^3}{L^3}-1\right\} & \text{for } L<\delta_m \\ \dfrac{V_z^0}{\overline{\rho}(z,T)}\left\{\dfrac{3(z-\delta_m+L)^2}{\delta_m^2}+\dfrac{2(z-\delta_m+L)^3}{\delta_m^3}-1\right\} & \text{for } L\geqslant\delta_m \text{ and } z\leqslant(\delta_m-L) \\ -V_z^0 \quad \text{for } L\geqslant\delta_m \text{ and } z>(\delta_m-L), \end{cases} \tag{18}$$

where $\overline{\rho}(z,T)$ is given by Eqs. (9) and (13). For $L<\delta_m$, the two approximate velocity equations are similar to the creep flow solutions for forced flow against a disk described by Chapman and Bauer [11], the principal difference being the temperature-dependent reduced density term $\overline{\rho}(z,T)$.

In Fig. 6 we compare the approximate analytical expression for the axial velocity profile and the exact calculation for two different sets of flow conditions. The analytical expressions developed above appear to be good approximations to the exact solutions in the temperature range 600 K$<T_d$ $<$1400 K and with V_z^0, L, and ω related by Eq. (12).

The approximations used in Eqs. (9) and (18) were chosen primarily for their simplicity. One shortcoming particular to the approximations being used above is that the analytical expressions do not compare as well to exact results in the vicinity of $L\sim\delta_T$. To see this, we plot the exact radial velocity profiles for three different L's and the new analytical expression [Eq. (18)] in Fig. 7. The behavior is consistent with the fact that the linear temperature approximation is a poor approximation in the vicinity of $L\sim\delta_T$ (see Fig. 4). A better approximation would improve the situation. For example, $T_0+\Delta T^*[1-(L+z)/\delta_T]^2$ turns out to be a reasonable approximation for $L\geqslant\delta_T$. Thus it is possible to obtain better approximations than Eqs. (9) and (18) for certain flow situations. However, in general, we have found these two approximations are reasonable for a fairly wide set of flow conditions.

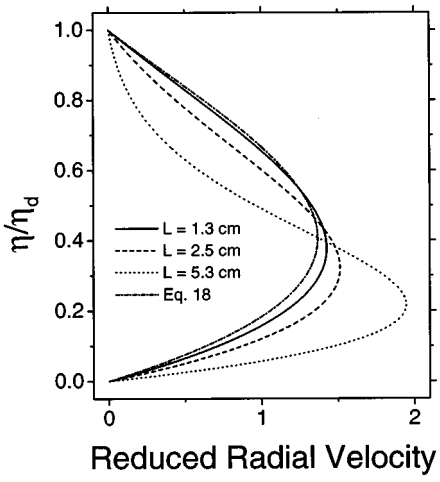

FIG. 7. Approximate analytical solutions and exact solutions to the governing equations for the reduced radial velocity profile, given by $V_r/(r^*V_z^0/L)$ with $\partial P/\partial r=0$. The simulated flow conditions are for hydrogen gas with $P=152$ torr, $V_z^0=10.6$ cm/sec, T_d $=1000$ K, and $T_0=400$ K. Under these conditions, the boundary layer thickness is approximately $\delta_m=5.3$ cm.

V. DISCUSSION

The above example for flow against a heated rotating disk demonstrates how one can combine a variable property stream function with a similarity variable transform to create a new variable property similarity transform. This reformulation technique should be applicable to other existing similarity transforms for which the stream function approach is appropriate. Using the stream function, and thereby the mass continuity equation, the functional and/or its spatial derivative can be related to at least two flow velocities. This, in turn, means that four boundary conditions can be applied to the determination of the functional and/or its spatial derivative. This is adequate to obtain a reasonable spatial approximation for the functional by a suitable analytical equation. In order to obtain variable property velocity approximations with this approach, it is necessary to also approximate the density profile. Since this is a reformulation of an existing transform, the temperature profiles have already been reported in most cases. Depending on the assumed relationship for P, ρ, T, the density profile can be deduced from the temperature profile shape. With the functional and the density profile approximation, it is then possible to obtain analytical velocity profiles that closely approximate the correct temperature behavior.

The temperature-dependent behavior in the axial direction is the primary difference between the method presented herein and previous approximate methods (e.g., Ref. [12]) for solving the flow governing equations. The importance of the temperature-dependent axial variations can be seen by inspection of the exact solutions in Fig. 2. An average property analytical approximation, for example, would not be able to predict the velocity increase near the injector (η/η_d ~0) caused by gas heating from the disk. The new approximate method, on the other hand, will show the spatial varia-

tion behavior one would expect for a system with a temperature gradient present (e.g., Fig. 6).

A. Flow stability criteria

Including the temperature effects in the analytical velocity approximations opens up a new path for examining thermal flow stability. Both the approximate analytical solutions and the exact solutions obtained using similarity transforms simulate a real fluid accurately only as long as the assumptions used to obtain the similarity transform remain valid. Convection-induced recirculation is an example of a fluid flow in which the similarity transform assumptions will no longer be valid. Thus, from both a fundamental and a practical standpoint, one would like a simple set of rules that determines the range of validity of the similarity transform to model a real, finite system. Historically, hydrodynamic stability has been studied theoretically using the linear analysis approach developed by Rayleigh. In this approach the effects of small disturbances to the steady-state governing equations are studied. The system is said to be stable if the disturbances decay to zero and unstable otherwise. Various approximate stability rules have been developed from the dimensionless variables appearing in the disturbance equations. The Rayleigh number, for example, has been shown experimentally to predict the onset of fluid convection in a cold-ceiling, hot-floor closed container. However, this method cannot be applied to every flow situation, including the case for axisymmetric stagnation point flow [13].

The approximate analytical equations developed above provide a new approach to stability analysis which we now sketch. The first step in this approach is to substitute the approximate analytical velocity profiles [Eq. (18)] and the temperature profile [Eqs. (9) and (13)] into the axial (gravity direction) momentum equation [Eq. (2)]. The result is a temperature-dependent analytical function for each term in the momentum equation. Any number of thermal stability criteria expressions can be developed from combinations of the various terms. By examining exact solution plots of the different terms in Eq. (2) for the heated rotating disk, we have determined that the primary contributions to the total axial momentum come from the gravity term ρg and the viscosity term, $\mu \partial^2 V_z / \partial z^2$. The two approximate terms were then integrated from the top of the thermal boundary layer to the middle of the boundary layer. For the $L > \delta_T$ flow regime, the ratio of the resulting terms is

$$FSP \sim \frac{8g(\Delta T/T_0)[T_d/(T_d+3T_0)]}{\omega\sqrt{\nu_0\omega}(T_{\text{ave}}/T_0)^{n+1}}. \tag{19}$$

Thermal stability will presumably be assured as long as *FSP* is smaller than some number that we are currently attempting to determine by comparing to experimental results. For this purpose, we are performing finite element calculations that mimic the flow situation depicted in Fig. 1.

The *FSP* parameter is similar to the *MCP* parameter used by Breiland and Evans [9] to study flow stability in a rotating heated disk system. For this flow regime, the stability predictions are expected to be essentially similar. For the $L < \delta_T$ flow regime, the ratio of the two approximate terms yields a different expression with L^2 dependence. The experimental verification of these various stability criteria expressions is too preliminary at this point to report. However, the results thus far are encouraging. We plan to present the complete theoretical derivations and results will be elsewhere [14].

B. Heated rotating disk applications

The above analysis of the flow against a heated disk has practical applications. Vertical flow, rotating disk systems are widely used in industry for chemical vapor deposition (CVD) because the model predicts uniform deposition. A CVD reactor operated so that $\partial P/\partial r \sim 0$ is one case in which the experimental flows can be made to closely approximate the theoretical flow. In this flow situation, the radial velocity is essentially zero right up to the boundary layer. This flow situation is advantageous since there will be minimal sidewall effects. Inside the boundary layer, radial velocities can become quite large. However, since the boundary layer thickness for most CVD reactor conditions is only a few centimeters at most, the only concern would be sidewall interactions over these few centimeters. From the analysis given above, a few dimensionless parameters can be used to determine when the reactor is being operated in this regime. For the forced flow against a heated rotating disk flow model (Fig. 1), we define a new dimensionless length β,

$$\beta \equiv \frac{L}{\delta_T} \cong \frac{L V_z^0 \sqrt{\text{Pr}}}{6\nu_0 H^2(\infty)\sqrt{T_d/T_0}}, \tag{20}$$

where Eq. (13) is used for the boundary layer thickness value δ_T. Furthermore, we define the Reynolds number as

$$\text{Re} \equiv \begin{cases} \dfrac{V_z(0,T)}{\omega L} & \text{for } \beta < 1 \\ \dfrac{V_z^2(0,T)}{6\omega\nu_0} & \text{for } \beta > 1. \end{cases} \tag{21}$$

Defined in this way, the Reynolds number will be consistent in the vicinity of $\beta \sim 1$. For $\beta > 1$, the flow behaves like infinite rotating disk flow if $\text{Re} \sim \frac{1}{6}$ [see Eq. (13)] and forced flow against a disk if $\text{Re} \gg \frac{1}{6}$. The fact that infinite rotating disk flow occurs at low Reynolds numbers explains why the velocity approximations [Eq. (18)] obtained above are similar to the creep flow solutions (i.e., $\text{Re} \sim 0$) described by Chapman and Bauer [11]. For $\beta < 1$, the flow behaves like forced flow in a channel for $\text{Re} \geqslant \frac{1}{6}$. For $\text{Re} < \frac{1}{6}$, there will be areas of radial inflow in the vicinity of the injector regardless of the value of β [4,7].

VI. CONCLUSION

We have presented a method for reformulating existing similarity transforms into new variable property similarity transforms. The new transforms are useful for developing approximate analytical solutions, and from these, the development of approximate flow stability parameters. To demonstrate the new transform and its usefulness, we applied the reformulation technique to axisymmetric fluid flow against a

heated rotating disk. Using a newly developed thermal boundary layer expression applicable to flow against a heated rotating disk, we obtained approximate analytical expressions for the velocity and temperature profiles that compare well with exact calculations. The reformulation technique for similarity transforms should be widely applicable to other similarity transforms that have appeared in the literature.

[1] C. Houtman, D. Graves, and K. Jensen, J. Electrochem. Soc. **133**, 961 (1986).
[2] D. S. Dandy and J. Yun, J. Mater. Res. **12**, 1112 (1997).
[3] M. Hitchman and B. Curtis, J. Cryst. Growth **60**, 43 (1982).
[4] D. Weyburne and B. Ahern, J. Cryst. Growth **170**, 77 (1997).
[5] T. von Kármán, Z. Angew. Math. Mech. **1**, 233 (1921).
[6] *Laminar Boundary Layers*, edited by L. Rosenhead (Dover, New York, 1963), pp. 156–162.
[7] G. Evans and R. Greif, Numer. Heat Transfer **14**, 373 (1988).
[8] H. Schlichting, *Boundary Layer Theory*, 6th ed. (McGraw-Hill, New York, 1968).
[9] W. Breiland and G. Evans, J. Electrochem. Soc. **138**, 1806 (1991).
[10] Note that linear fits are better for ω versus $V_z^0/L^{1.3}$ plots. However, the use of this correlation would require inclusion of a dimensioned constant whose value depends on the type of gas. The correlation used in Eq. (12) is not as good for large V_z^0/L values, but appears to work for all the gases we have studied.
[11] T. Chapman and G. Bauer, Appl. Sci. Res. **31**, 223 (1975).
[12] See, for examples of approximate solution methods, discussion in Ref. [6], Chap. 6.
[13] K. Chen, M. Chen, and C. Sohn, J. Fluid Mech. **132**, 49 (1993).
[14] D. Weyburne (unpublished).